This document was prepared in conjunction with work accomplished under Contract No. DE-AC09-96SR18500 with the U. S. Department of Energy.

DISCLAIMER

WSRC-TR-2005-00241
Revision 0

BASELINE MICROSTRUCTURAL CHARACTERIZATION OF OUTER 3013 CONTAINERS

PHILIP E. ZAPP AND KERRY A. DUNN

SAVANNAH RIVER NATIONAL LABORATORY

Publication Date: July, 2005

Westinghouse Savannah River Company
Savannah River Site
Aiken, SC 29808

PREPARED FOR THE U.S. DEPARTMENT OF ENERGY UNDER CONTRACT DE-AC09-96SR18500

WSRC-TR-2005-00241
Revision 0

SMT
STRATEGIC MATERIALS TECHNOLOGY

Keywords:
Stainless Steel
Metallography
Microhardness

BASELINE MICROSTRUCTURAL CHARACTERIZATION OF OUTER 3013 CONTAINERS

Philip E. Zapp and Kerry A. Dunn

Issued

July, 2005

_____ Date: _____
Authorized Derivative Classifier

SRNL SAVANNAH RIVER NATIONAL LABORATORY, AIKEN, SC 29808
Westinghouse Savannah River Company
Prepared For The U.S. Department Of Energy Under Contract DE-AC09-96SR18500

DOCUMENT: WSRC-TR-2005-00241 Revision 0

TITLE: **BASELINE MICROSTRUCTURAL CHARACTERIZATION OF OUTER 3013 CONTAINERS**

APPROVALS

_____ Date: _____
P. E. Zapp, Author
Materials Technology Section

_____ Date: _____
K. A. Dunn, SRNL Pu Surveillance Program Lead and Author
Materials Technology Section

_____ Date: _____
B. J. Wiersma, Technical Reviewer
Materials Technology Section

_____ Date: _____
J. W. McClard, MIS Representative
NMM Facility Engineering

_____ Date: _____
G. T. Chandler, Manager
Materials Performance and Corrosion Technology

_____ Date: _____
N.C. Iyer, Manager
Materials Technology Section

WSRC-TR-2005-00241
Revision 0

Distribution:

H. A. Gunter, 703-H
S. D. Burke, 705-K
K. J. Durrwachter, 705-K
P. A. Leeper, 707-C
J. W. McClard, 703-H
R. J. Martini, 704-9K
K. A. Dunn, 773-41A
N. C. Iyer, 773-41A
G. T. Chandler, 773-A
P. E. Zapp, 773-A
R. R. Livingston, 773-A
MTS Records, c/o L. Hillary, 773-41A

BASELINE MICROSTRUCTURAL CHARACTERIZATION OF OUTER 3013 CONTAINERS

SUMMARY

Three DOE Standard 3013 outer storage containers were examined to characterize the microstructure of the type 316L stainless steel material of construction. Two of the containers were closure-welded yielding production-quality outer 3013 containers; the third examined container was not closed. Optical metallography and Knoop microhardness measurements were performed to establish a baseline characterization that will support future destructive examinations of 3013 outer containers in the storage inventory. Metallography revealed the microstructural features typical of this austenitic stainless steel as it is formed and welded. The grains were equiaxed with evident annealing twins. Flow lines were prominent in the forming directions of the cylindrical body and flat lids and bottom caps. No adverse indications were seen. Microhardness values, although widely varying, were consistent with annealed austenitic stainless steel. The data gathered as part of this characterization will be used as a baseline for the destructive examination of 3013 containers removed from the storage inventory.

INTRODUCTION

The DOE 3013 storage standard specifies two nested, welded stainless steel containers to store plutonium-bearing materials for up to 50 years.[1] The outer of the two containers is fabricated of 316L stainless steel. Figure 1 is a photograph of a 3013 outer can, indicating the fabrication weld which joins the drawn body of the can to the bottom cap and the closure weld which joins the lid to the body. Two of three examined containers were closure-welded yielding production-quality outer 3013 containers. There are two closure weld techniques used in the DOE complex: laser weld and gas tungsten arc weld. The third examined container was not closed and was used for confirmation of parent-metal microstructure.

Type 316L stainless steel is an iron-based, austenitic (face-centered-cubic crystal structure) alloy with 16 - 18% chromium, 10 – 14% nickel, 2 - 3% molybdenum, and 0.03% carbon. The high chromium content imparts corrosion resistance through the formation of a thin, adherent chromium oxide layer. The nickel is necessary to maintain the tough and ductile austenite phase against transformation to the less ductile ferrite phase. Molybdenum is added for additional corrosion resistance; it especially contributes to resistance to chloride-induced corrosion. The low carbon level of < 0.035% precludes the precipitation of chromium carbides along grain boundaries when the steel is heated, as in conventional welding, to high temperatures. (Formation of these carbides depletes the steel matrix of the corrosion-preventing chromium.) Austenitic stainless steels in the 300 series of the American Iron and Steel Institute's numbering system are substitutional alloys (alloy elements substitute for iron in the crystal lattice) consisting microstructurally of a single phase. They cannot be strengthened through heat treatment

(by precipitating particles or grains of a second phase), but can be strengthened only by cold working (deformation at low temperature).

Although austenitic stainless steels cannot be strengthened through heat treatment, cold-worked stainless steel can be softened through the process of annealing, in which residual stresses are relieved by heating the material. The engineering property of hardness quantifies the degree of hardening or softening these materials. Hardness is the measure of the resistance of a material to indentation by a stylus under load. For the measurement of metallographically sectioned laboratory specimens, a small pyramidal diamond stylus or indenter is often used; the term microhardness is applied to values resulting from the use of the Knoop or Brinell diamond indenters.

Microstructural information as revealed by optical metallography and microhardness data can be used to characterize engineering materials of construction. This document provides a baseline characterization of the 3013 outer container, in accordance with the task technical plan.[2] A wide range of metallographic images are presented here. This information will support destructive examinations of 3013 outer cans and aid in identifying any anomalies in future observations of containers in storage. The data reported here have been recorded in Laboratory Notebook WSRC-NB-2002-00180.

CHARACTERIZATION

Three 3013 outer cans were examined for this report. Figure 1 is a photograph of an outer can identical to those examined. Specimens from each can were cut and mounted according to standard metallographic laboratory procedures. The specimens were electrolytically etched in a 10% oxalic acid solution in order to reveal the grain structure of the stainless steel. Microhardness was measured with a Knoop microhardness tester, M&TE number 89005, on the metallographically prepared specimens. A load of 100 grams was used in the hardness testing.

Can number 1 had serial number R602363 and had a TIG weld for the closure weld. Can number 1 was the most thoroughly examined and serves as the reference can for future comparisons. Metallographic specimens were cut from the lid, bottom cap, three locations on the cylindrical body, and from four locations of the closure weld. Can number 2, serial number P00318 had a closure weld made with a laser process. The lid, closure weld, body, and bottom cap were examined. Can number 3, serial number PS0390, was not closure welded. Only the lid, body, and bottom cap were examined.

Optical Metallography

The optical metallography performed on the 3013 cans consisted of bright-field images from magnification of 50X to 500X. As a solid-solution, single-phase alloy, 316L stainless steel displays a simple microstructure of low photographic contrast. The microstructure of the parent (not welded) 316L stainless steel in the cans consists predominantly of equiaxed (regularly shaped) grains with some annealing twins. (Twins are regions within a grain whose crystal lattices are mirror images of one another. They

appear metallographically as parallel light and dark bands.) This microstructure is typical of austenitic stainless steel.[3]

A marked feature in the metallography of the 3013 can is the texture imparted by the methods of forming the components of the can. The components of the can were formed by rolling (lid and bottom cap) or by drawing (body). These forming methods are revealed in low-magnification metallography as contrasting dark flow lines running parallel to the forming direction. The flow lines are created by the deformation of non-metallic inclusions in the steel and grains with favored crystallographic orientations with respect to the forming direction.

Representative micrographs of can 1 are shown in Figures 2 through 13. Figures 2 and 3 show a section of the body of can 1 that was cut parallel to the can axis. The flow lines created in the forming process of the body are clearly evident. The black spots in these (and following) micrographs are etch pits (holes created by the electrolytic reaction with the 10% oxalic acid) nucleated at dispersed carbide particles. Figures 4 and 5 are micrographs of sections of the can 1 body cut perpendicular to the can axis, that is across rather than with flow lines. Figures 6 and 7 and figures 8 and 9 are images of the can 1 lid and bottom cap, respectively. These components are formed from rolled sheet and therefore show the familiar flow line pattern. Annealing twins are particularly prominent in Figure 9. The fabrication weld and the closure weld of can 1 are shown in Figures 10 and 11 and Figures 12 and 13, respectively. The multiple passes of the TIG weld process are evident in the solidified weld metal, which contrasts sharply with the adjacent parent metal. Flow lines of the can 1 body are prominent in Figure 13, but not visible in this particular section of the can 1 lid.

Figures 14, 15, and 16 are micrographs of the laser closure weld of can 2, which is distinguished from the TIG weld of can 1 by the absence of the contrast of multiple passes. The fabrication weld of can 2 is identical in microstructural features to the can 1 fabrication weld (Figures 17, 18, and 19). The parent metal microstructure of the can 2 body is shown in Figures 20 and 21; the can 2 microstructure is identical to that of can 1, as expected. Figures 22 and 23 show the microstructure of the can 2 lid and bottom cap, respectively, with prominent flow lines and annealing twins as in can 1.

The metallography of can 3 is shown in Figures 24 and 25 for the lid, and Figures 26 through 30 for the can body. The microstructural features seen in the base metal of cans 1 and 2 are again seen in the examination of can 3. Features not previously detected, however, are the small voids of no structural significance, originating in the casting of the steel, seen in a section of the can 3 body (Figures 29 and 30).

Knoop Microhardness

Metal hardness values of metallographically prepared specimens are often quoted in the Knoop hardness scale. Knoop microhardness data obtained from cans 1, 2, and 3 are listed in Table 1. Typical hardness values range from about 160 to about 220, with a few values falling outside this range. There appears to be wide variation in the hardness data,

even from a single mounted specimen (e.g., specimen 1-1 or 1-6). These Knoop hardness values are similar to Rockwell B hardness values of 78 to 93. Handbook values of stainless steel hardnesses are frequently quoted in Rockwell B or C scales. Annealed 316L stainless steel has a maximum Rockwell B hardness of 95.[3] Thus the wrought outer can material tests at lower hardness than handbook values for annealed sheet or plate. Note in Table 1 that Knoop hardness values of weld material exceed those for the parent material.

CONCLUSIONS

Metallography of three 3013 outer cans fabricated from 316L stainless steel revealed the microstructural features typical of this austenitic stainless steel as it is formed and welded. The grains were equiaxed with evident annealing twins. Flow lines were prominent in the forming directions of the cylindrical body and flat lids and bottom caps. No adverse indications were seen. Microhardness values, although widely varying, were consistent with annealed austenitic stainless steel.

ACKNOWLEDGEMENTS

The authors acknowledge Elise Labord, Bridget Miller, and Angela Bowser for optical metallography and microhardness measurements.

REFERENCES

1. DOE-STD-3013-2004, “Stabilization, Packaging, and Storage of Plutonium-Bearing Materials.”

2. K. A Dunn, “Task Technical Plan for Baseline Microstructural Characterization of Outer 3013 Containers (U),” WSRC-RP-2002-00190, March 2002.

3. *Metals Handbook*, 8th Edition, ASM International, Materials Park, Ohio, 1972.

Table 1 Knoop Microhardness Values

Can Number 1:
R602363

Specimen	1 - 1:	Bottom cap center	
Location	A	B	C
Measurement 1	180.1	187.2	195.3
Measurement 2	180.3	199.6	205
Measurement 3	181.8	194.4	204.4
Averages	180.7	193.7	201.6

Specimen	1- 2A:	Bottom cap to body TIG weld		
Location	Bottom parent metal	Bottom HAZ	Body HAZ	Weld
Measurement 1	211.4	159.4	183.6	176.4
Measurement 2	216.7	162.6	190.6	179.8
Measurement 3	219.7	167.6	189.3	186.2
Averages	215.9	163.2	187.8	180.8

Specimen	1 - 3:	Body lower half	
Location	A	B	C
Measurement 1	170.2	183.6	173.7
Measurement 2	166.8	173.4	172.1
Measurement 3	165.4	176.8	169.4
Averages	167.5	177.9	171.7

Specimen	1 - 4:	Body mid height	
Location	A	B	C
Measurement 1	168.7	169.7	178.6
Measurement 2	177.5	165.4	164.6
Measurement 3	173.4	176.8	167.9
Averages	173.2	170.6	170.4

Specimen	1 - 5:	Body upper half	
Location	A	B	C
Measurement 1	183.8	172.5	174.5
Measurement 2	184.2	168.1	175
Measurement 3	177.9	174.5	171.2
Averages	182.0	171.7	173.6

Specimen	1 - 6:	Lid center	
Location	A	B	C
Measurement 1	191.3	163.5	167.1
Measurement 2	197.9	158	164.8
Measurement 3	191.2	160.6	166.3
Averages	193.5	160.7	166.1

Specimen	1 - 7:	Lid to body TIG weld			
Location	Lid parent metal A	Lid parent metal B	Lid HAZ	Body HAZ	Weld
Measurement 1	153.7	171.5	171.8	180.1	198.3

Measurement 2	153.2	163.5	165.8	187.8	192.1
Measurement 3	161.3	163.5	168.5	185.2	189.3
Averages	156.1	166.2	168.7	184.4	193.2

Can Number 2:
H000318

Specimen 2 - 1: Cut from lid; lid to body laser weld 90 degree

Location	Lid parent metal	Lid HAZ	Weld A	Weld B	Weld C	Body HAZ	Body parent metal	Body parent metal
Measurement	196.5	206	205.4	204.2	219.9	203.1	201.4	220.5

Specimen 2 - 2: Bottom cap center

Measurement 1	201.4
Measurement 2	192.8
Measurement 3	236.7
Average	210.3

Specimen 2 -3: Fabrication Weld

Location	Bottom parent metal	Bottom HAZ	Weld A	Weld B	Weld C	Body HAZ	Body parent metal
Measurement	180.8	184.7	208.3	247.7	193.3	188.2	189.2

Specimen 2 -4: Lid center

Measurement 1	158.1
Measurement 2	193.8
Measurement 3	178
Average	176.6

Can number 3: PS0930

Location	Lid A	Lid B	Side A	Side B	Bottom A	Bottom B
Measurement 1	188.1	188.5	160.7	176.1	179.9	187
Measurement 2	162.9	184	164.7	171.2	178.6	180.4
Measurement 3	186.4	170.9	193.4	168.6	187.5	187
Averages	179.1	181.1	172.9	172.0	182.0	184.8

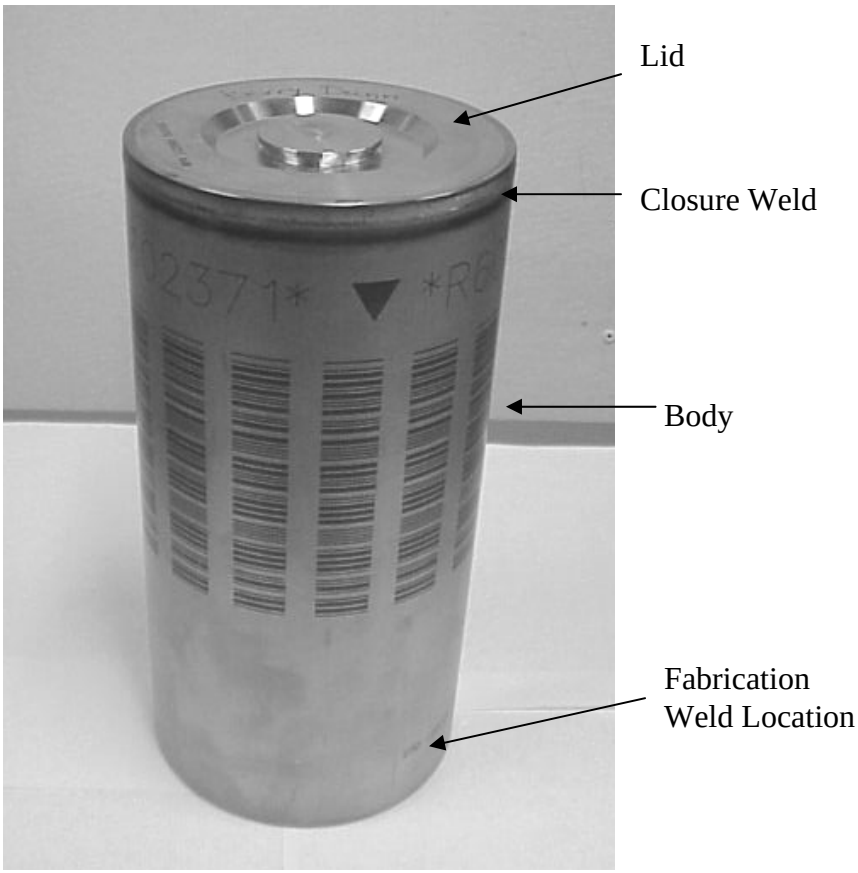

Figure 1 Photograph of a 3013 outer can.

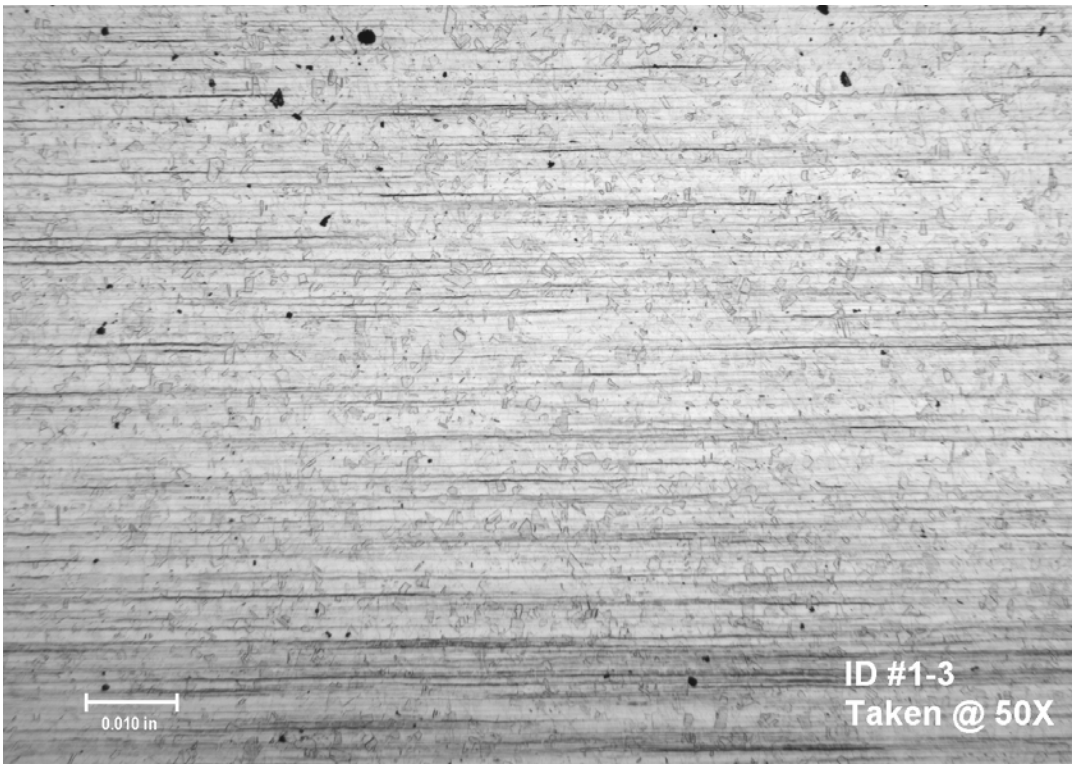

Figure 2 Micrograph of body of can 1 at 50X magnification. Section parallel to can axis, with prominent flow lines.

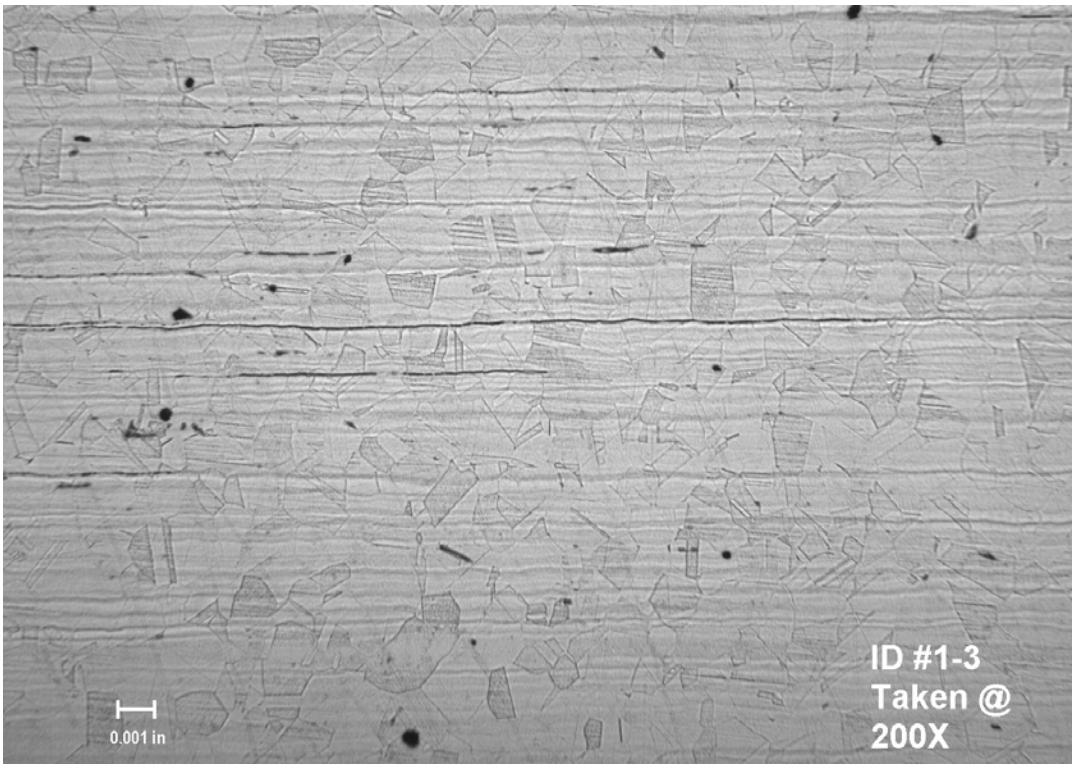

Figure 3 Micrograph of body of can 1 at 200X magnification.

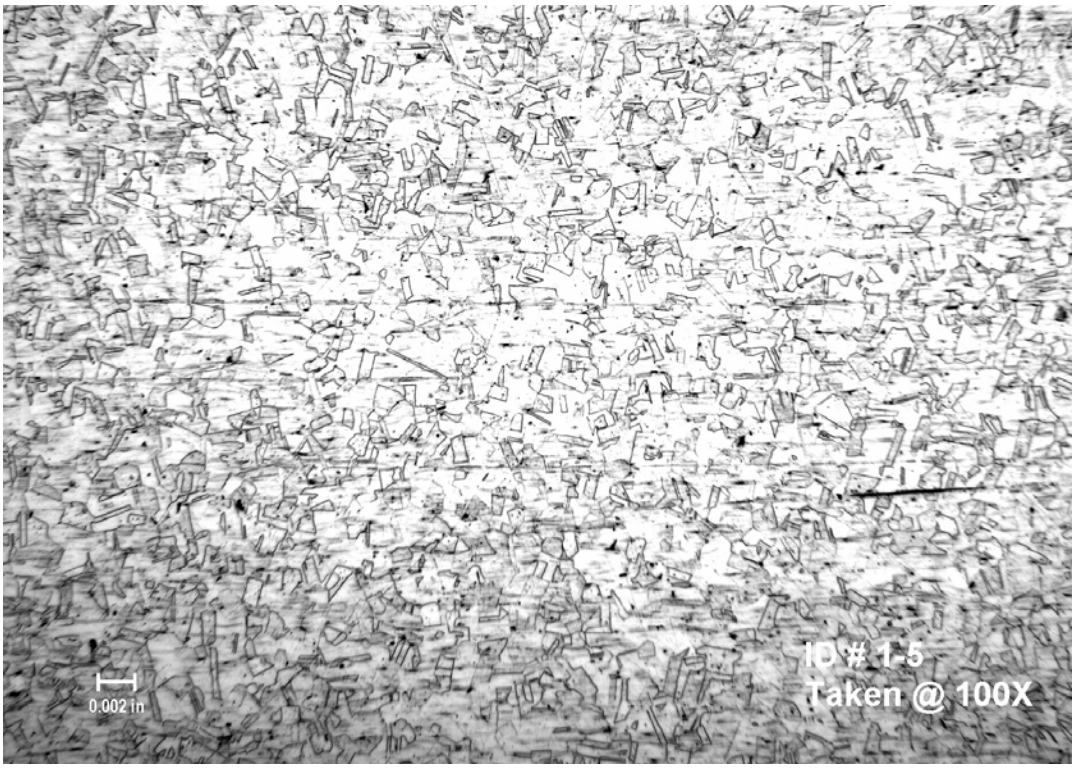

Figure 4 Micrograph of body of can 1 at 100X magnification. Section perpendicular to can axis, flow lines mostly absent.

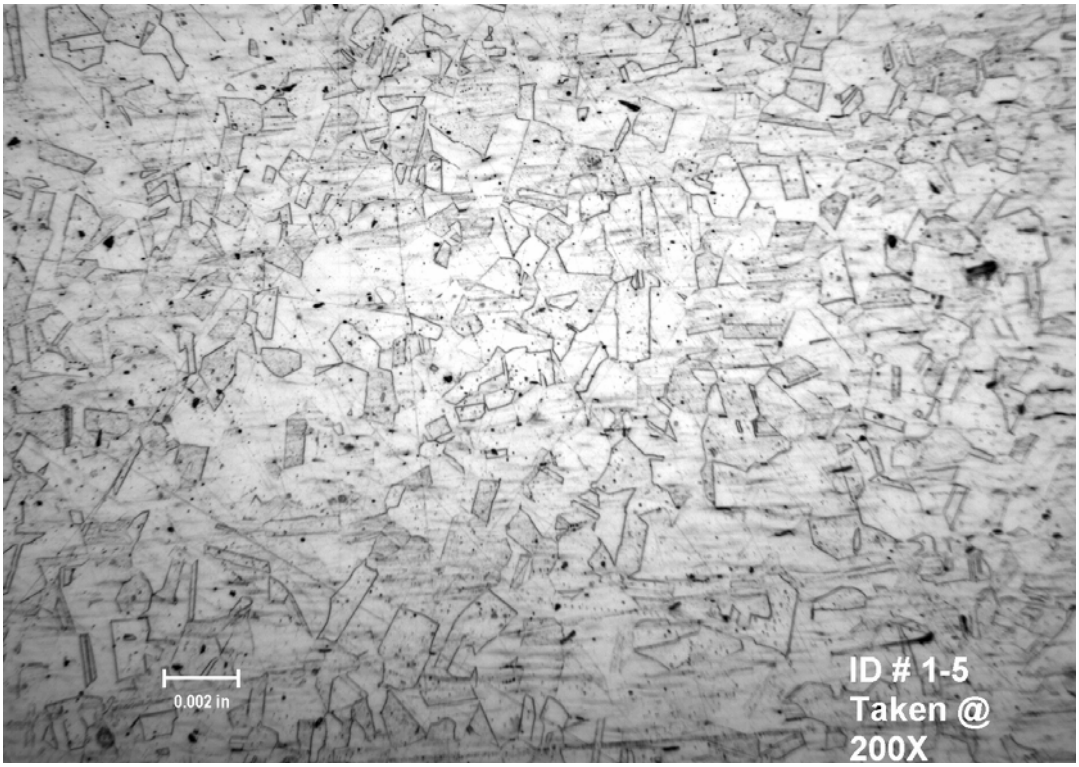

Figure 5 Micrograph of body of can 1 at 200X magnification. Section perpendicular to can axis.

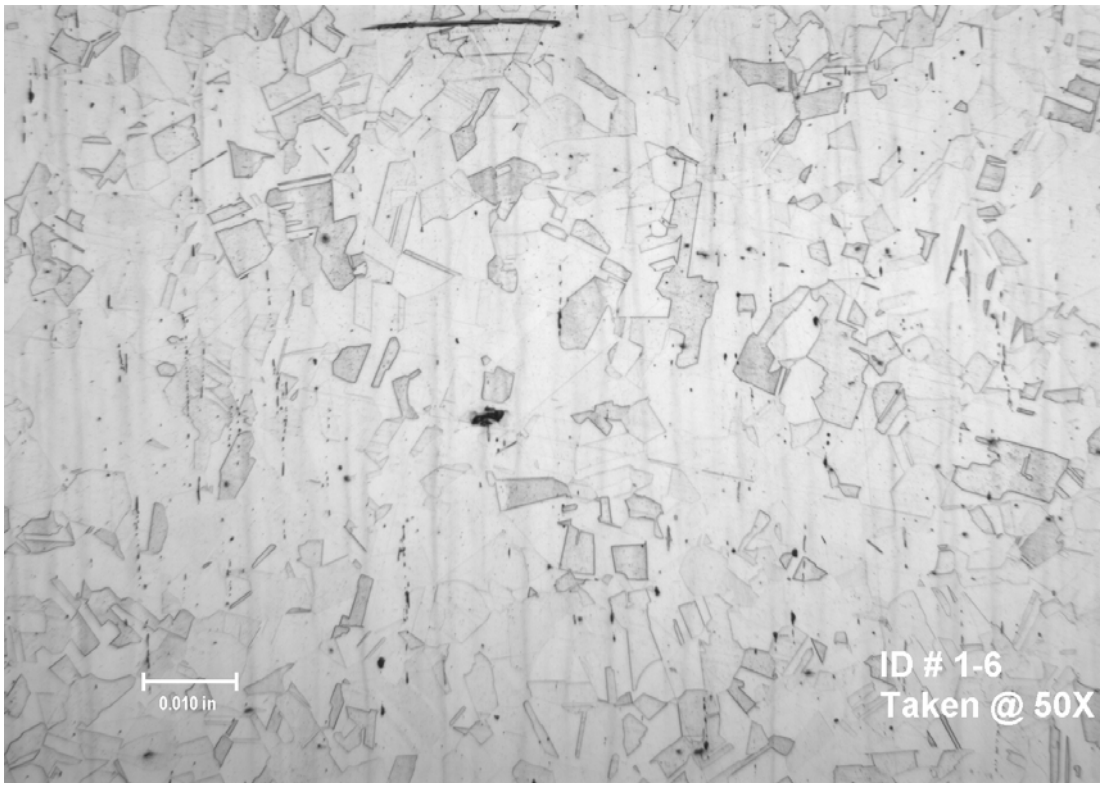

Figure 6 Micrograph of lid of can 1 at 50X magnification. Section in plane of lid.

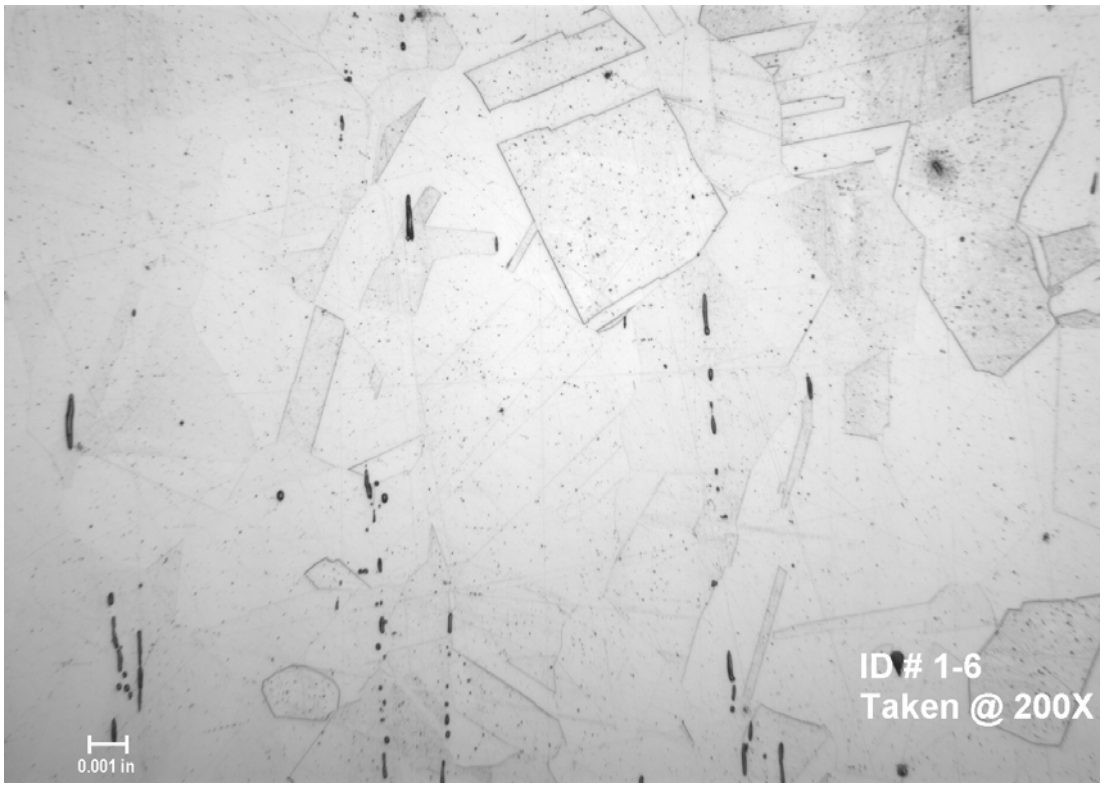

Figure 7 Micrograph of lid of can 1 at 50X magnification. Section in plane of lid.

Figure 8 Micrograph of bottom cap of can number 1.

Figure 9 Micrograph of bottom cap of can 1 at 200X magnification. Annealing twins prominent in large grain.

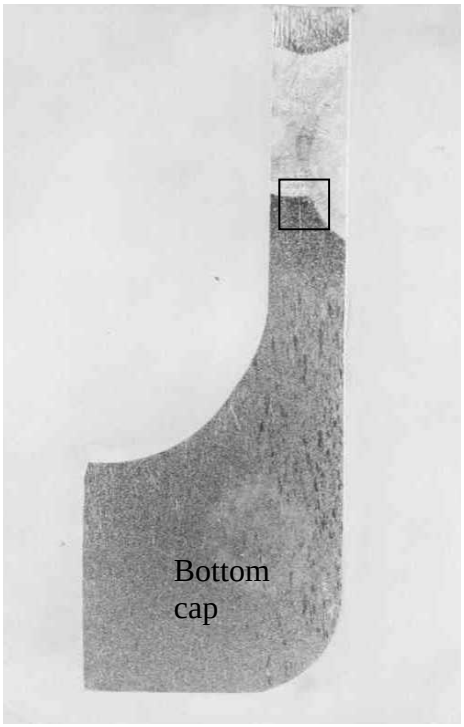

Figure 10 Metallographic section of bottom cap of can 1 showing fabrication weld. Area within box enlarged in Figure 11.

Figure 11 Portion of fabrication weld of can 1 at 50X magnification.

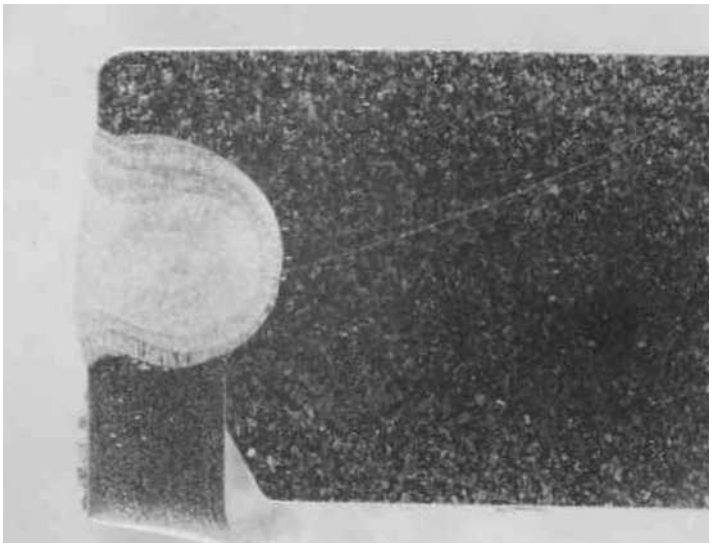

Figure 12 Metallographic section of closure weld of can 1.

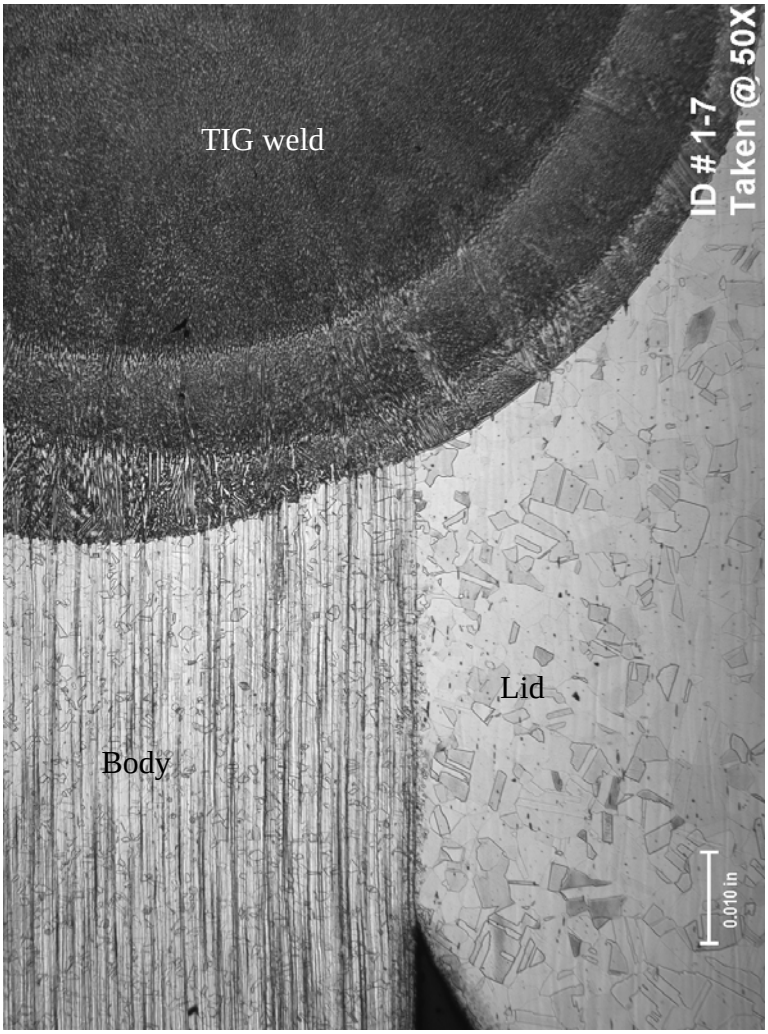

Figure 13 Portion of closure weld of can 1 at 50X magnification.

Figure 14 Section of closure weld of can 2 by laser process.

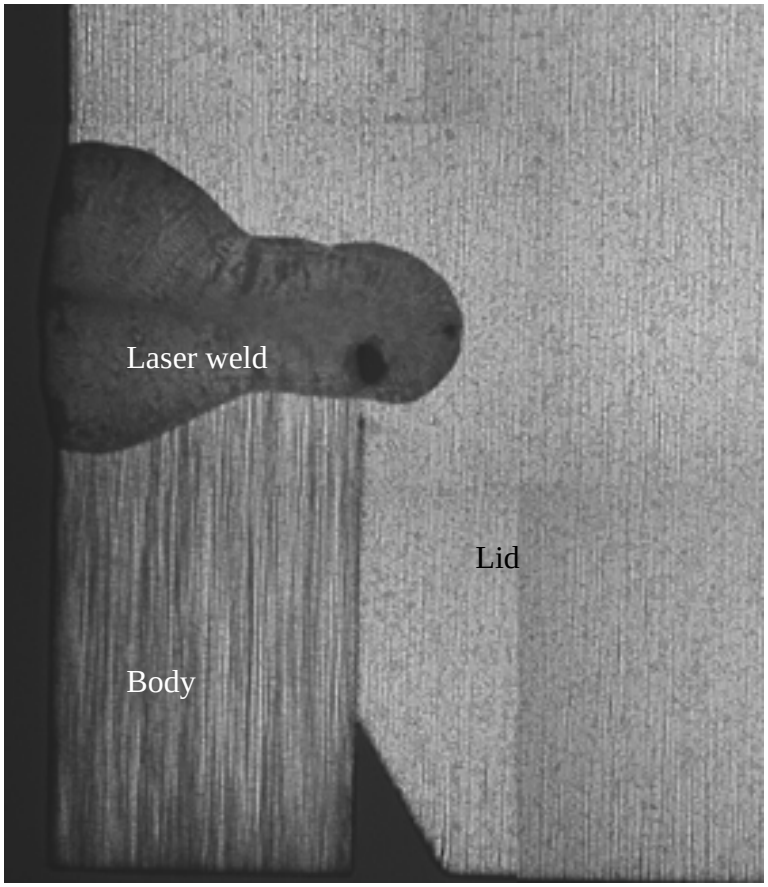

Figure 15 Composite micrograph of closure weld of can 2.

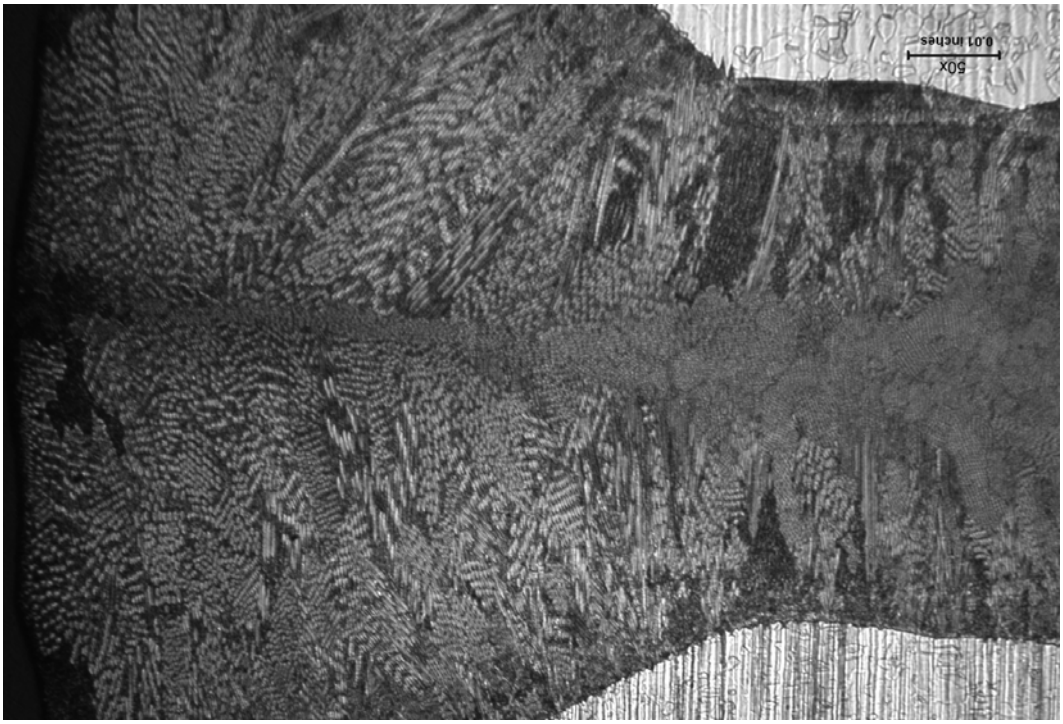

Figure 16 Section of can 2 laser weld at 50X magnification.

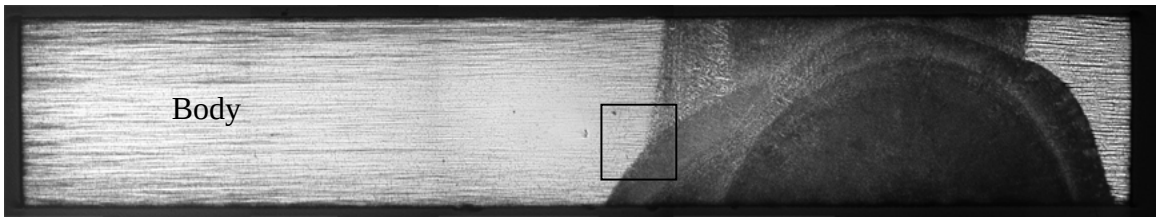

Figure 17 Composite micrograph of fabrication weld of can 2. Area within box enlarged in Figure 18.

Figure 18 Section of fabrication weld of can 2 at 50X magnification.

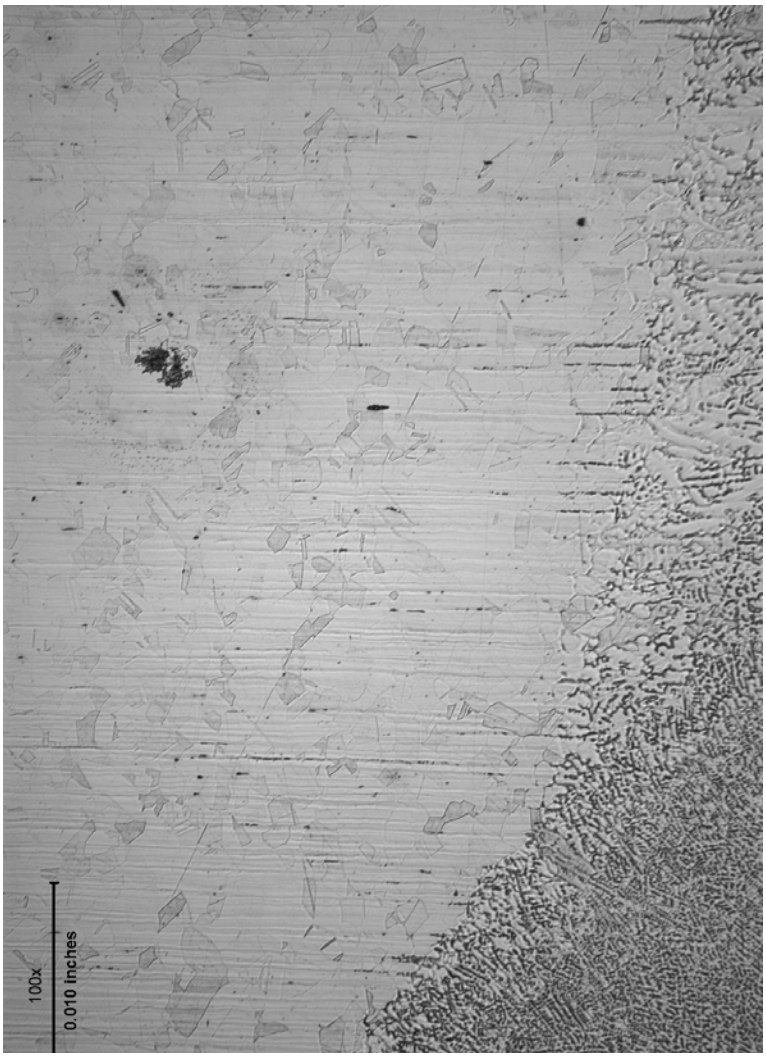

Figure 19 Edge of fabrication weld of can 2 at 100X magnification

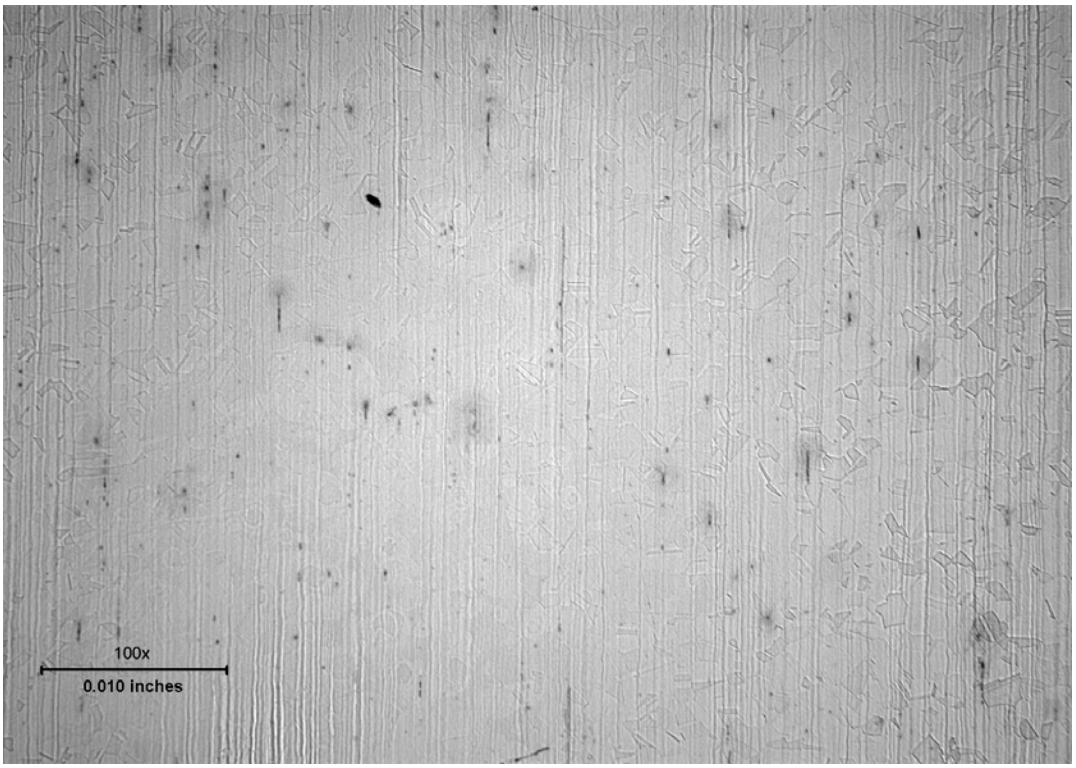

Figure 20 Micrograph of can 2 body at 100X magnification. Flow lines and etch pits evident.

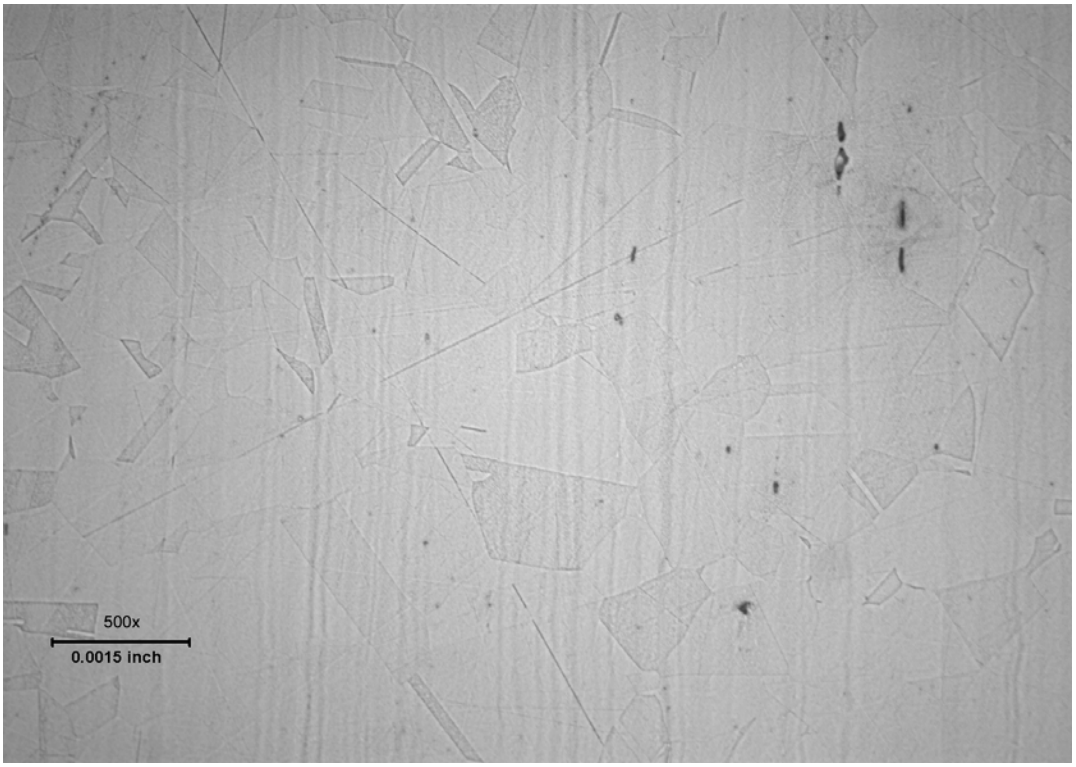

Figure 21 Micrograph of can 2 body at 500X magnification. Flow lines and etch pits evident.

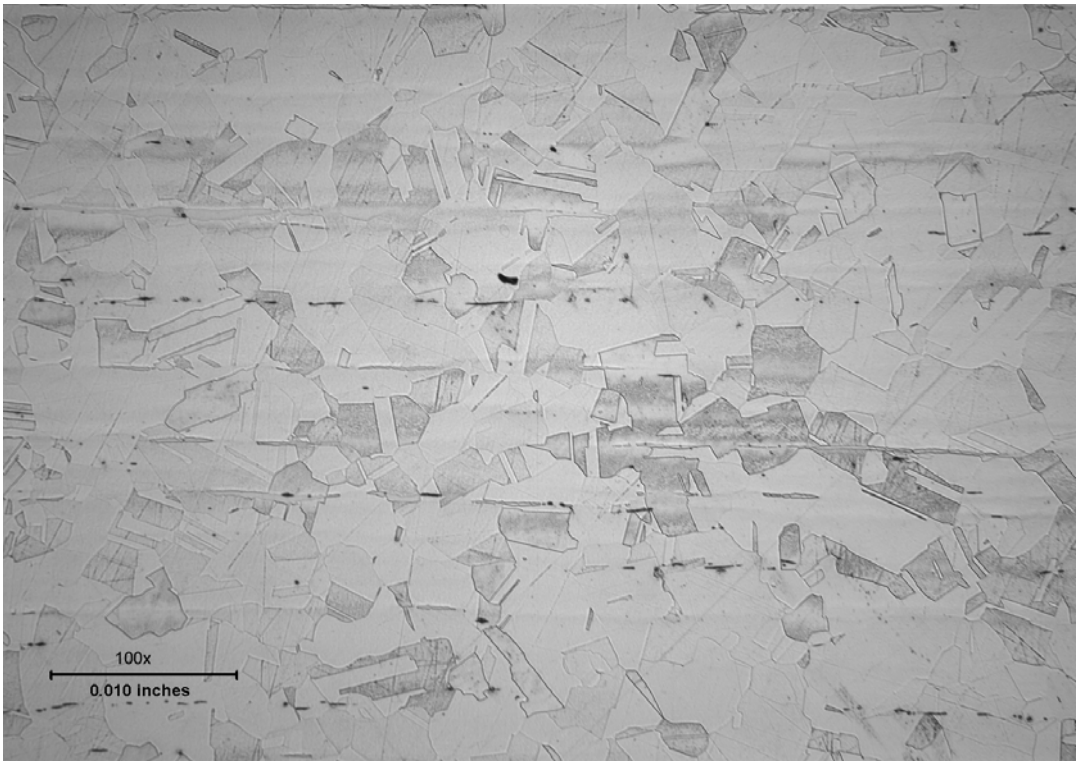

Figure 22 Micrograph of can 2 lid at 100X magnification.

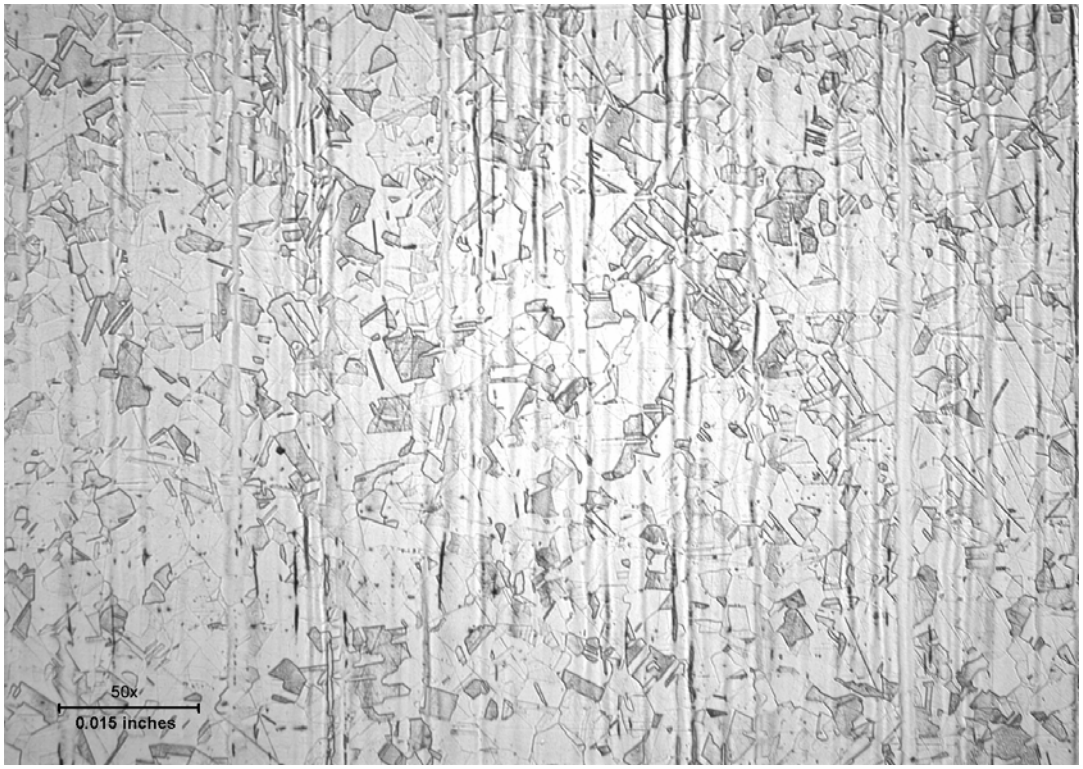

Figure 23 Micrograph of can 2 bottom cap at 50X magnification, with prominent flow lines.

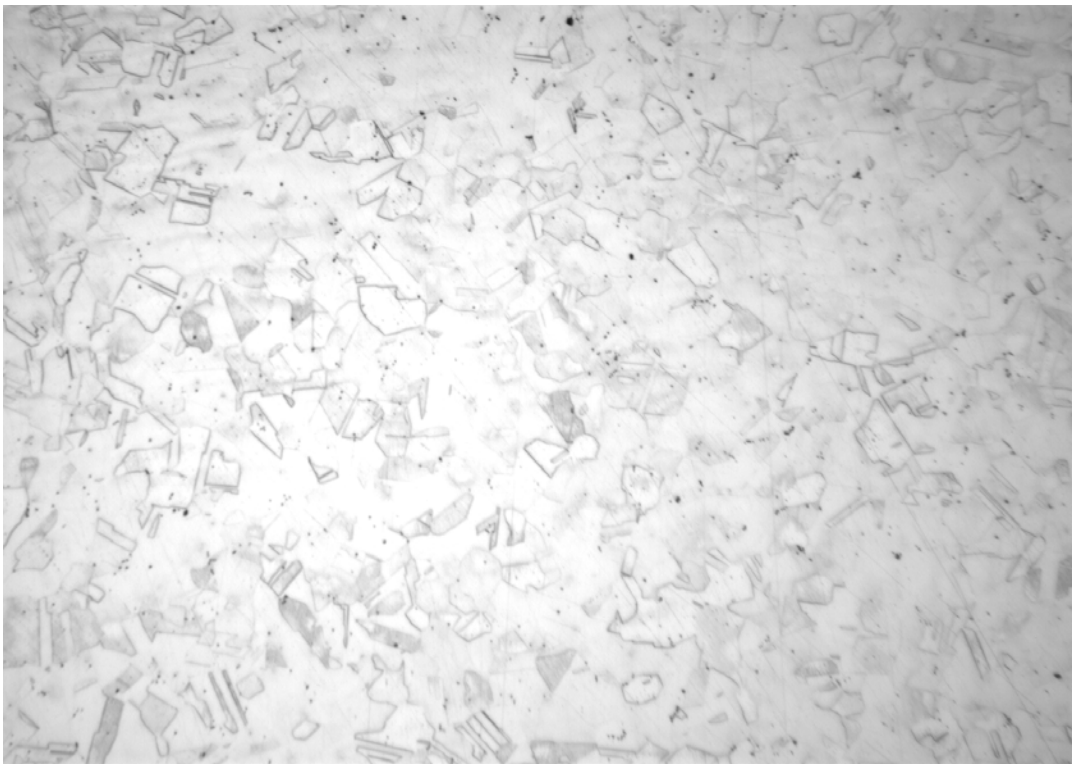

Figure 24 Micrograph of lid of can 3 at 100X magnification.

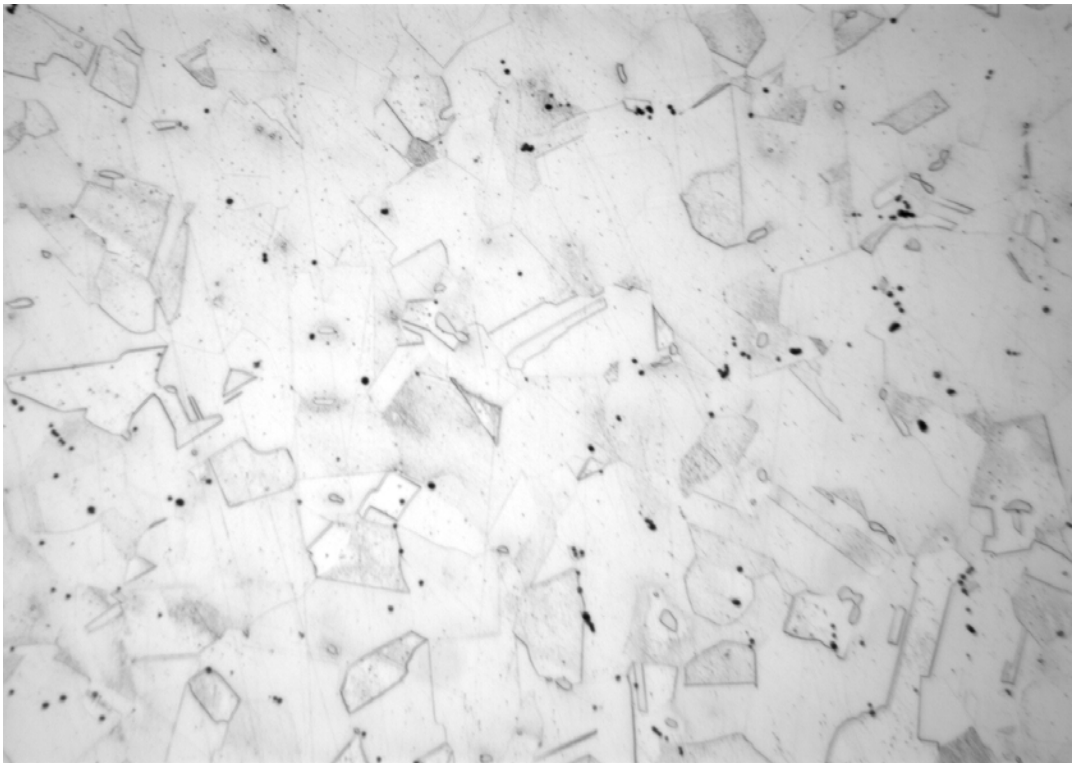

Figure 25 Micrograph of lid of can 3 at 250X magnification.

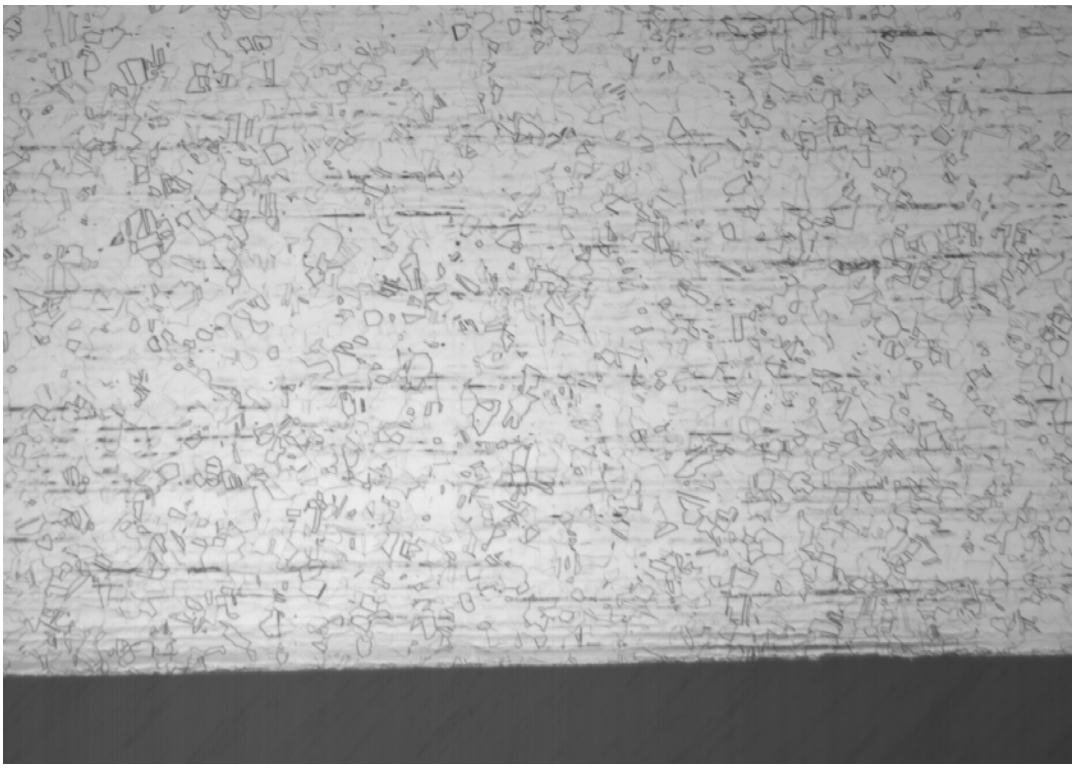

Figure 26 Micrograph of body of can 3 at 50X magnification. Section parallel to can axis.

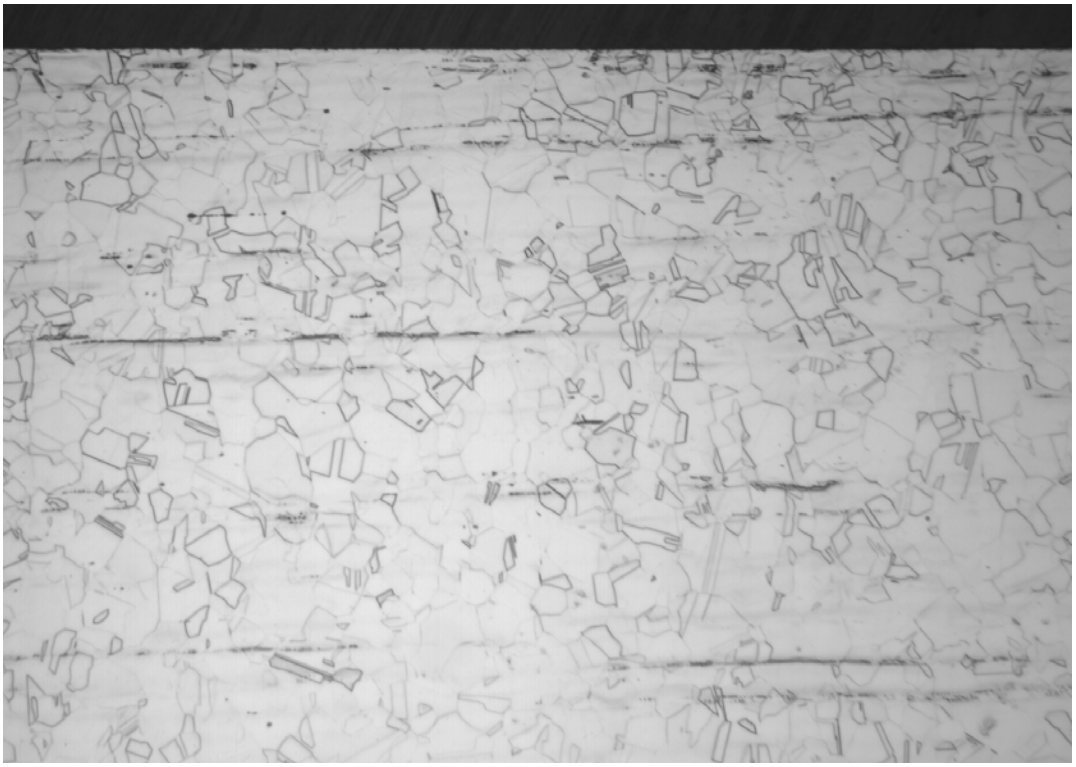

Figure 27 Micrograph of body of can 3 at 100X magnification. Section parallel to can axis.

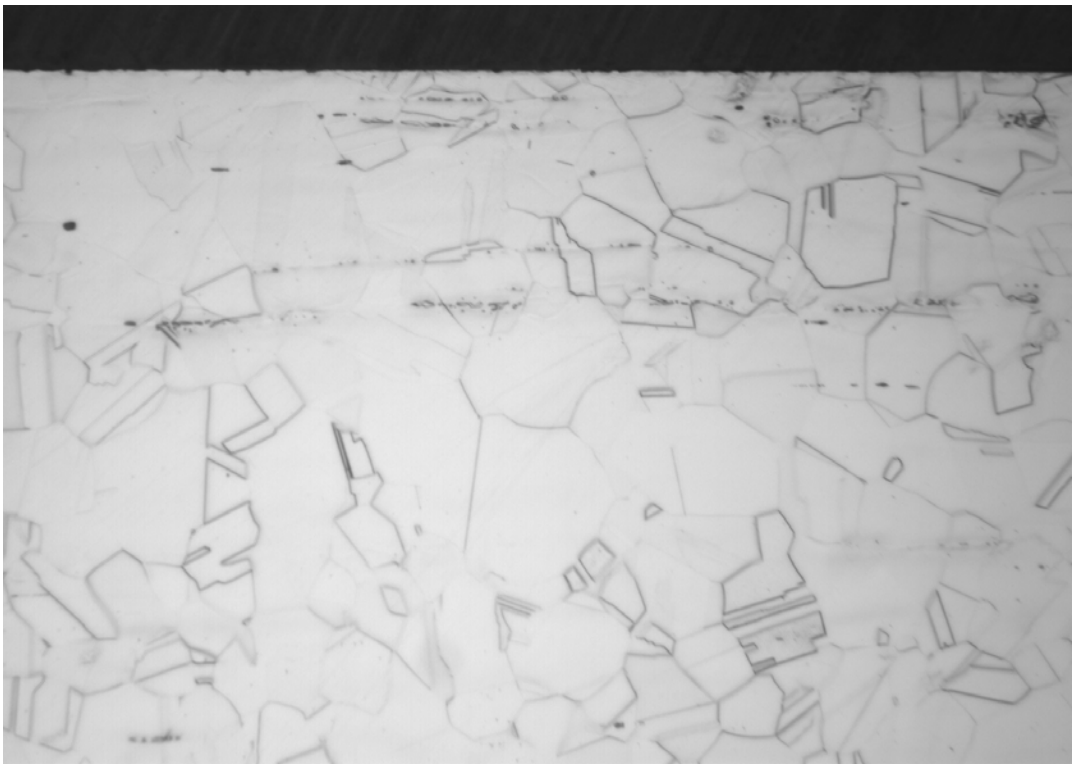

Figure 28 Micrograph of body of can 3 at 250X magnification. Section parallel to can axis.

Figure 29 Micrograph of body of can 3 at 20X magnification. Section perpendicular to can axis.

Figure 30 Micrograph of body of can 3 at 100X magnification. Section perpendicular to can axis.